

Beyond the acceptance limit of DRAGON: the case of the ${}^6\text{Li}(\alpha, \gamma){}^{10}\text{B}$ reaction

A. Psaltis^a, A. A. Chen^a, D. S. Connolly^b, B. Davids^b, G. Gilardy^{c,d}, R. Giri^h, U. Greife^e, W. Huang^{b,f}, D. A. Hutcheon^b, J. Karpesky^e, A. Lennarz^b, J. Liang^a, M. Lovely^e, S. N. Paneru^h, C. Ruiz^b, G. Tenkila^g, M. Williams^{b,1}

^aDepartment of Physics and Astronomy, McMaster University, Hamilton, Ontario L8S 4M1, Canada

^bTRIUMF, 4004 Wesbrook Mall, Vancouver, British Columbia V6T 2A3, Canada

^cDepartment of Physics, Joint Institute for Nuclear Astrophysics, University of Notre Dame, Notre Dame, Indiana 46556, USA

^dCentre d'Études Nucléaires de Bordeaux Gradignan, UMR 5797 CNRS/IN2P3 - Université de Bordeaux, 19 Chemin du Solarium, CS 10120, F-33175 Gradignan, France

^eDepartment of Physics, Colorado School of Mines, Golden, Colorado 80401, USA

^fPhysics Department, University of Northern British Columbia, Prince George, BC V2N 4Z9, Canada

^gDepartment of Physics and Astronomy, University of British Columbia, Vancouver, British Columbia V6T 1Z4, Canada

^hDepartment of Physics, and Astronomy, Ohio University, Athens, Ohio 45701, USA

ⁱDepartment of Physics, University of York, Heslington, York YO10 5DD, United Kingdom

Abstract

Radiative capture reactions play a pivotal role for our understanding of the origin of the elements in the cosmos. Recoil separators provide an effective way to study these reactions, in inverse kinematics, and take advantage of the use of radioactive ion beams. However, a limiting factor in the study of radiative capture reactions in inverse kinematics is the momentum spread of the product nuclei, which can result in an angular spread larger than the geometric acceptance of the separator. The DRAGON facility at TRIUMF is a versatile recoil separator, designed to study radiative capture reactions relevant to astrophysics in the $A \sim 10\text{--}30$ region. In this work we present the first attempt to study with DRAGON a reaction, ${}^6\text{Li}(\alpha, \gamma){}^{10}\text{B}$, for which the recoil angular spread exceeds DRAGON's acceptance. Our result is in good agreement with the literature value, showing that DRAGON can measure resonance strengths of astrophysically important reactions even when not all the recoils enter the separator.

Keywords: recoil separators, inverse kinematics, radiative capture, resonance strength

1. Introduction

Radiative capture reactions involving hydrogen and helium are of pivotal importance for nuclear astrophysics. Knowing their cross sections improves reaction network calculations and thus our predictions for the origin of the elements in the universe. Given that these reactions involve the two most abundant elements in the cosmos, they occur in almost any astrophysical scenario, including quiescent (*e.g.* Ne–Na, Mg–Al cycles) and explosive (*e.g.* rp -process, νp -process) stellar burning. These reactions are traditionally studied using intense proton and α -beams from low-energy accelerators, impinging onto a heavy target. This technique, even though it is still used until today with great success, has some drawbacks, such as the beam induced background and the inability to use short-lived targets. Using recoil separators, radiative capture reactions can

be studied in inverse kinematics, with a heavy ion beam (stable or radioactive) impinging on a gas target (usually hydrogen or helium). Their advent remedies the aforementioned problems, but imposed some new ones, mainly of a geometric nature [1, 2].

The Detector of Recoils and Gammas of Nuclear reactions (DRAGON) facility in the Isotope Separator and Accelerator–I (ISAC–I) experimental hall at TRIUMF, Canada's particle accelerator centre in Vancouver, BC has carried out many of the radiative capture measurements involving radioactive ion beams to date. Even though it was constructed to study reactions with beams up to $A=30$ [3, 4], over the last two decades, DRAGON has demonstrated versatility, having performed experiments from $A=3$, *e.g.*, ${}^3\text{He}(\alpha, \gamma){}^7\text{Be}$ [5], to $A=76$, *e.g.*, ${}^{76}\text{Se}(\alpha, \gamma){}^{80}\text{Kr}$ [6].

The experiment presented in this work is a proof of the capability of DRAGON to measure resonant cross sections of radiative capture reactions of astrophysical interest in which the angular cone of the recoils ex-

Email address: psaltisa@mcmaster.ca (A. Psaltis)

Table 1: List of some astrophysically important reactions in the $A = 7 - 24$ mass region. The Q -value of each reaction is presented in MeV, along with the astrophysical scenario that it affects and the respective energy region of the Gamow window in the center of mass system (E_{cm}). The $\theta_{r,\text{max}}$ value for each reaction is the maximum angle the recoils can have in the Gamow window listed in the second column. The reactions marked with \star have been measured using the DRAGON recoil separator, but not necessarily in the Gamow window, and the reactions marked with \dagger have an angular cone greater than DRAGON's maximum acceptance $\theta_{\text{DRAGON}} = \pm 21$ mrad. See text for details.

Reaction	Q value (MeV) E_{cm} (MeV)	Astrophysical Scenario (nucleosynthesis process)	$\theta_{r,\text{max}}$ (mrad)
${}^7\text{Li}(\alpha, \gamma){}^{11}\text{B}^\dagger$	8.664 0.7–3.6	Core–Collapse Supernovae ν -process	± 51
${}^7\text{Be}(\alpha, \gamma){}^{11}\text{C}^\dagger$	7.544 0.5–1.2	Core–Collapse Supernovae νp -process	± 44
${}^7\text{Be}(p, \gamma){}^8\text{B}$	0.136 0.02	Sun pp -chains (solar ν)	± 3
${}^{12}\text{C}(\alpha, \gamma){}^{16}\text{O}^{\dagger\star}$	7.162 0.03	Intermediate mass/Massive stars Quiescent helium burning	± 138
${}^{13}\text{N}(p, \gamma){}^{14}\text{O}$	4.626 0.3–2.2	X-ray bursts hot CNO cycle	± 15
${}^{15}\text{O}(\alpha, \gamma){}^{19}\text{Ne}$	3.528 1.5–4.6	X-ray bursts hot-CNO cycle	± 21
${}^{16}\text{O}(\alpha, \gamma){}^{20}\text{Ne}^{\dagger\star}$	4.730 0.02	Intermediate mass/Massive stars Quiescent helium burning	± 87
${}^{17}\text{O}(\alpha, \gamma){}^{18}\text{F}^\dagger$	7.348 0.1–0.5	AGB stars, massive stars, and novae s -process	± 64
${}^{18}\text{O}(\alpha, \gamma){}^{22}\text{Ne}^\dagger$	9.667 0.6–2.3	Intermediate mass/Massive stars s -process	± 55
${}^{20}\text{Ne}(\alpha, \gamma){}^{24}\text{Mg}$	9.316 0.04	Intermediate mass/Massive stars Quiescent helium burning	± 105
${}^{22}\text{Ne}(p, \gamma){}^{23}\text{Na}^\star$	8.794 0.3–0.5	AGB stars/ classical novae Ne–Na cycle	± 18
${}^{22}\text{Ne}(\alpha, \gamma){}^{26}\text{Mg}^\dagger$	10.614 0.038–1.450	Intermediate mass/Massive stars s -process	± 105
${}^{23}\text{Mg}(p, \gamma){}^{24}\text{Al}^\star$	1.863 0.5–0.9	O–Ne–Mg novae Ne–Na cycle	± 3

ceeds its geometric acceptance. It was selected as a benchmark for the measurement of unknown resonance strengths of the ${}^7\text{Be}(\alpha, \gamma){}^{11}\text{C}$ reaction, which is important for νp -process nucleosynthesis (see Table 1). In the past, there have been acceptance-challenging experiments for nuclear reaction studies with DRAGON, such as the ${}^{12}\text{C}({}^{16}\text{O}, \gamma){}^{28}\text{Si}$ and ${}^{12}\text{C}(\alpha, \gamma){}^{16}\text{O}$, reported in References [7, 8], but these studies did not involve the measurement of a resonance strength. For this test we used a known resonance at a center of mass energy of $E_r = 1458.5(6)$ keV of the ${}^6\text{Li}(\alpha, \gamma){}^{10}\text{B}$ reaction whose strength was originally measured by Forsyth *et al.* in forward kinematics [9]. The present measurement was performed in inverse kinematics, using a sta-

ble ${}^6\text{Li}$ beam provided by the TRIUMF Off-Line Ion Source (OLIS) [10].

The paper is structured as follows: in Section 2 we give a brief overview of conducting experiments using recoil separators and the challenges of studying reactions with low mass ion beams. In Section 3 we discuss the measurement by Forsyth *et al.*. In Section 4 we give an overview of DRAGON and the experimental setup, in Section 5 we present the data analysis and the results, and finally in Section 6 we present our conclusions by discussing the final results in more detail.

2. Radiative capture reactions using recoil separators

Radiative capture reactions in inverse kinematics occur in a usually gaseous target, at rest in the laboratory frame, with the entire laboratory momentum being carried by the beam. The compound nucleus is formed in an excited state with energy

$$E_x = E_{cm} + Q \quad (1)$$

where E_{cm} is the energy in the center of mass system, and when the reaction proceeds through a resonance, $E_{cm} = E_r$. $Q = (m_1 + m_2 - m_3)c^2$ is the reaction Q value, where m_1, m_2 and m_3 are the masses of the projectile, the target, and the recoil, respectively.

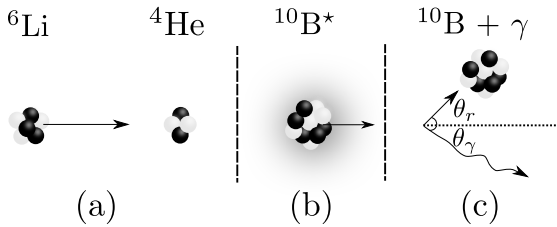


Figure 1: Schematic representation of a radiative α -capture on ${}^6\text{Li}$ in inverse kinematics: (a) beam (${}^6\text{Li}$) and target (${}^4\text{He}$) particles interact, (b) the compound nucleus (${}^{10}\text{B}$) is synthesised in an excited state and then, (c) it decays by emitting a γ ray. The recoil nucleus and the γ ray are emitted in angles θ_r and θ_γ in the lab system respectively. See the text for details.

The excited nucleus decays by emitting one or multiple γ rays ($\sum_i E_{\gamma_i} = E_x$), which carry some of the initial momentum, and thus the products (recoil nuclei) form a narrow cone centered on the beam direction (see Figure 1). In the simple case of a single γ transition to the ground state, perpendicular to the beam direction ($\theta_\gamma = \pi/2$), the maximum angle of the recoil nucleus can be calculated to be:

$$\theta_{r,max} \approx \arctan \left(\frac{Q + E_{cm}}{\sqrt{2m_1 c^2 \left(\frac{m_1 + m_2}{m_2} \right) E_{cm}}} \right) \quad (2)$$

A similar relation to Equation 2 can also be derived for the momentum spread of the recoils, $\Delta p/p$. The minimum of both relations appears at $E_{cm} = Q$. This behaviour is very interesting, since in the astrophysically relevant energy region, reactions with $Q/E_{cm} < 1$ have increasing $\theta_{r,max}$ with increasing energy, while reactions with $Q/E_{cm} > 1$ exhibit the opposite behaviour. For example, the ${}^7\text{Be}(p, \gamma){}^8\text{B}$ reaction, with a Q value of 136.4 keV can be a very challenging measurement for

resonances with $E_r > Q$, since $\theta_{r,max}$ increases with increasing energy [1]. On the other hand, for resonances with $E_r \sim 1$ MeV, typical for astrophysical environments, the ${}^6\text{Li}(\alpha, \gamma){}^{10}\text{B}$ (Q -value = 4461.19 keV), has a decreasing $\theta_{r,max}$ with increasing energy, which is similar to the ${}^7\text{Be}(\alpha, \gamma){}^{11}\text{C}$ reaction (Q -value = 7543.6 keV), and for this reason is a good choice for a surrogate reaction. For a more detailed discussion regarding the kinematics formalism of radiative capture reactions using recoil separators for astrophysics the reader is referred to References [1, 2].

What is really important in the case of an experimental study is not the maximum cone angle of the recoils, but rather their angular distribution, which affects the number of recoils within a given angular range of zero degrees, ultimately defining the transmission efficiency of recoils through the separator. The recoil angular distribution depends on the γ cascade and more specifically on the γ branching ratios and the γ angular distribution. To illustrate the above statements, we show in Figure 2 how the recoil angular distribution of the $E_r = 1458.5(6)$ keV resonance of ${}^6\text{Li}(\alpha, \gamma){}^{10}\text{B}$ reaction can be affected by changing either the number of the γ rays in the cascade (left) or their angular distribution (right), which can be a M1/E2 decay from the $J = 2^+$ state to the $J = 1^+$ and $J = 3^+$ states. It is evident that a single transition to the ground state results in a distribution with a peak closer to the maximum angle $\theta_{r,max}$, while multiple γ rays shift the distribution to smaller angles. This behaviour affects both the recoil transmission through the separator and the efficiency of the γ ray detection system. As far as the γ angular correlations are concerned, for the case of radiative α capture on ${}^6\text{Li}$ in the center of mass system, the quadrupole distribution ($W(\theta) \propto \sin^2 \theta \cos^2 \theta$) shifts the average recoil momentum angle to smaller angles, compared to the uniform ($W(\theta) = 1$) and dipole ($W(\theta) \propto \sin^2 \theta$) cases, as we can see in Figure 2 – Right. Table 2 shows an overview of the GEANT simulation that we discussed in the above.

Recoil separators are built with an intrinsic angular acceptance, which sets a geometric limit to the number of reactions they can study. Table 1 shows an overview of some important astrophysical reactions and their respective recoil cone angles at energies relevant for astrophysics. For some of them the maximum momentum angle of the recoils is quite large (>30 mrad), posing a great challenge to study them in inverse kinematics using recoil separators. The reaction we selected to study in this work, ${}^6\text{Li}(\alpha, \gamma){}^{10}\text{B}$, has a maximum recoil angle of $\theta_{r,max} = \pm 32$ mrad at $E_{cm} = 1458.5(6)$ keV, which is 22 mrad greater than DRAGON's angular acceptance ($\theta_{DRAGON} = \pm 21$ mrad).

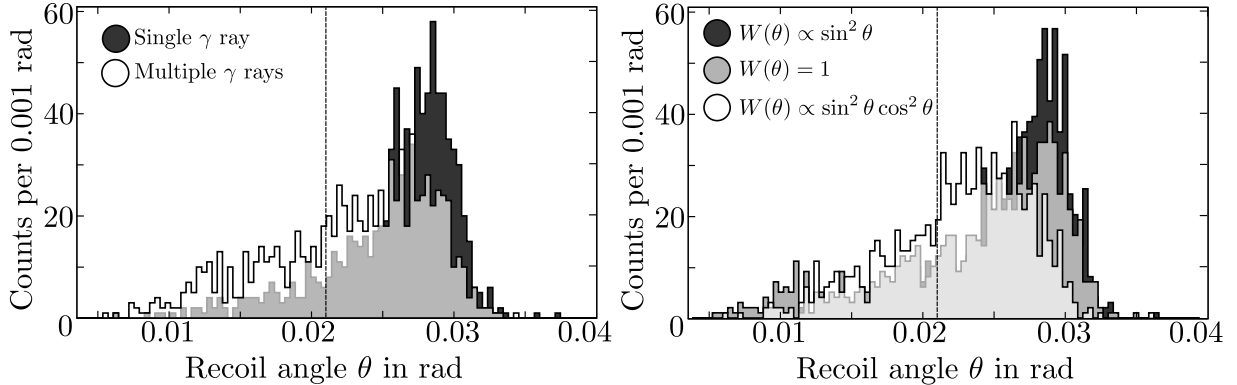


Figure 2: GEANT simulation results for the recoil angular distribution of the $E_r = 1458.5$ keV resonance of ${}^6\text{Li}(\alpha, \gamma){}^{10}\text{B}$ reaction by changing (*Left*) the number of γ rays emitted in the cascade and (*Right*) their angular distribution (**Dipole** - $W(\theta) \propto \sin^2 \theta$, **Uniform** - $W(\theta) = 1$ and **Quadrupole** - $W(\theta) \propto \sin^2 \theta \cos^2 \theta$.) The vertical line shows DRAGON's angular acceptance, ± 21 mrad. See the text for details.

Table 2: Tabulated results of the GEANT simulations presented in Figure 2. See the text for details.

# of emitted γ rays	γ angular distribution, $W(\theta)$	Separator transmission (%)	BGO efficiency (%)
1	Uniform	5.89 ± 0.83	73.58 ± 15.52
3	Uniform	27.4 ± 1.9	80.4 ± 7.6
2	Uniform	7.31 ± 0.93	69.7 ± 13.4
2	Dipole	11.86 ± 1.21	64.81 ± 9.95
2	Quadrupole	17.08 ± 1.48	73.25 ± 8.99

In cases like that, the planning of an experiment and the subsequent analysis relies heavily on detailed simulations of the separator (GEANT in the case of DRAGON) which provides information about the transmission of the recoils and the resonance energy. It is very useful to have a prior knowledge of the γ branching ratios and the γ angular distributions, but even in the case of a completely unknown γ cascade, simulations can be used to estimate the branching ratios [1].

3. Previous Measurement

The only published measurement of ${}^6\text{Li}(\alpha, \gamma){}^{10}\text{B}$ reaction's $E_r = 1458.5(6)$ keV ($E_x = 5919.5(6)$ keV) resonance strength was performed by Forsyth *et al.* [9]. The measurement was carried out at the University of Maryland Van de Graaff accelerator lab in regular kinematics, using a singly-charged ${}^4\text{He}$ beam ($E_\alpha = 0.9\text{--}3.3$ MeV & $I_\alpha = 2.5 \mu\text{A}$) and a 96% isotopically enriched ${}^6\text{Li}$ target. γ rays were detected using a NaI crystal placed at 90° with respect to the beam.

The resonance strength was found to be $\omega\gamma = 0.228(38)$ eV and its width $\Gamma = 6(1)$ keV in the center of mass system. Branching ratios of the γ transi-

tions were determined to be 82(5) % and 18(5) % to the ground state and the first excited state, respectively (see Figure 3), contrary to a single transition to the ground state reported in a study by Meyer-Schützmeister and Hanna [11]. The reported branching ratios were used as input for the GEANT simulations of DRAGON, which provided the recoil transmission and the BGO γ array detection efficiency (see Section 5.5).

4. Experimental Details

Our study was carried out in inverse kinematics using a beam of ${}^6\text{Li}^+$ from OLIS, which was accelerated through the ISAC-I Radio-Frequency Quadrupole (RFQ) and Drift-Tube Linac (DTL) to an average energy of 0.612(1) A MeV ($E_{lab} = 3.675(6)$ MeV, $E_{cm} = 1.468(3)$ MeV), so that the resonance was centered in the gas target. The beam energy spread was $\Delta E/E \leq 0.3$ % throughout the experiment [13], with an average intensity of $1.94 \times 10^{10} \text{ s}^{-1}$ (see also Section 5.2). The windowless gas target pressure was maintained at $P = 5.0(1)$ Torr, corresponding to a thickness of $1.97(4) \times 10^{18} \text{ atoms/cm}^2$. Choosing the aforementioned beam energy and gas target pressure, we were covering a

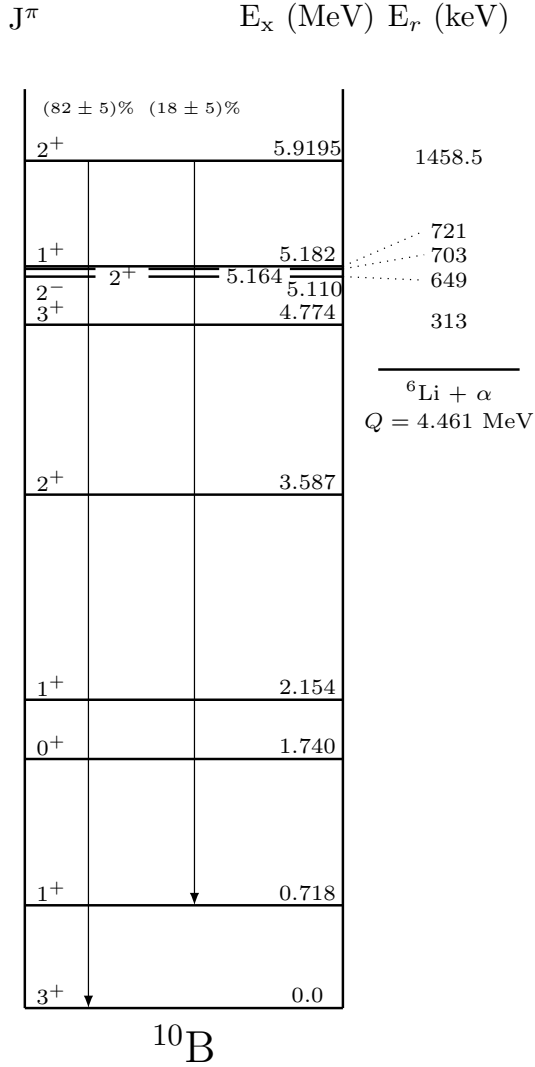


Figure 3: Partial level scheme of the low-lying energy levels of ${}^{10}\text{B}$. Two γ -transitions of the $E_x = 5919.5(6)$ keV state are shown. The reaction Q value was taken from AME2016 [12].

center-of-mass energy window of 1458.5 ± 10 keV. The most intense charge state of the recoils (${}^{10}\text{B}^{2+}$) was tuned through the separator to a $66 \mu\text{m}$ thick, gridded Double-Sided Silicon Strip Detector (DSSSD) placed near the focal plane of DRAGON with a typical rate of 15–20 Hz.

5. Data Analysis & Results

To extract the resonance strength and compare it to the literature value, we first had to calculate the reaction yield, which includes identifying the recoils, determining the total number of beam particles, measuring the charge-state fraction of the recoils, and calculating the efficiency of the BGO array as well as the transmission of the recoils through the separator using GEANT simulations.

5.1. Particle Identification

The ${}^{10}\text{B}$ recoils were detected by the DSSSD in coincidence with γ rays in the BGO array. Further discrimination was provided using software cuts on the separator time-of-flight (see Figure 6), which is defined as the time difference between a γ hit in a BGO detector and a hit in the DSSSD at the focal plane of DRAGON [14]. DRAGON is very efficient in rejecting unreacted beam ions for (α, γ) reactions, with demonstrated suppression factors of $> 10^{13}$, which can be increased by few orders of magnitude, by using the aforementioned software cuts [1, 5, 15].

5.2. Beam Normalization

To ensure a precise measurement of the reaction yield, we monitored the beam current throughout the experiment using Faraday cups located along DRAGON. In particular, the number of beam ions N_{beam} , impinging on the windowless gas target is calculated using the following method: a silicon surface barrier (SSB) detector placed at a well-defined lab angle of 57° inside the target was detecting the elastically scattered gas target particles during each run. For a time window $\Delta t \sim 240$ s, before and after each run, we recorded these measurements. At the same time, beam current measurements were made at a Faraday cup located 2 m upstream of the target. The normalized number of beam ions, N_{beam} , is then given by:

$$N_{beam} = \mathcal{R} N_\alpha \frac{E^2}{P} \quad (3)$$

where E is the beam energy and P is the gas target pressure. \mathcal{R} is the normalization coefficient, given by:

$$\mathcal{R} = \frac{I}{q|e|} \frac{\Delta t}{N_\alpha} \frac{P}{E^2} \eta_{trg} \quad (4)$$

where $I/|e|$ is the current reading at the aforementioned Faraday Cup in ions per second, η_{trg} is the beam transmission through an empty target, q is the charge state of the beam (1^+), and N_α is the number of scattered target (α) nuclei into the surface barrier detector during Δt .

5.3. Boron charge state distribution

Given that DRAGON is tuned to select and transport only a single recoil charge state to the final focal plane, it is necessary to measure the recoil charge state distribution (CSD) using a beam of an abundant isotope of the recoil element, to determine the total reaction yield. Charge State Distribution measurements were performed using a ^{11}B beam provided by OLIS. The results are compared with the semi-empirical formulae of Liu *et al.* [16] and Schiwietz & Grand [17] (see Figure 4).

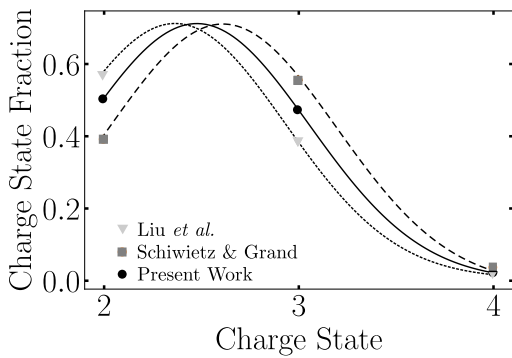


Figure 4: Comparison between the experimentally measured CSD (η_{CSD}) for ^{11}B with the semi-empirical formulae of Liu *et al.* [16] and Schiwietz & Grand [17]. The fit to the experimental data is a Gaussian function. The error bars are smaller than the size of the points.

5.4. ^6Li Stopping Power in ^4He

One of the advantages of studying reactions using recoil separators is that the stopping power ϵ , which is required for the calculation of the resonance strength, is measured directly and is not based on semi-empirical formulae, which introduce an additional uncertainty to the measurement, especially when they are extrapolated to low energies. At DRAGON, stopping powers are measured by varying both the pressure in the gas target and the magnetic field strength needed to centre the beam at a momentum dispersed angular focus in the focal plane of the first magnetic dipole of DRAGON (see Figure 5). We used these results to calculate the expected yield $Y_{\omega\gamma_0}$ in Equation 5 and compare our experimental results with GEANT simulations (see Section 5.5).

5.5. Log-likelihood analysis for E_r & $\omega\gamma$

The analysis of the BGO detector spectrum for the highest energy γ ray emitted by the de-excitation of the ^{10}B recoils (Figure 6) shows that the resonance

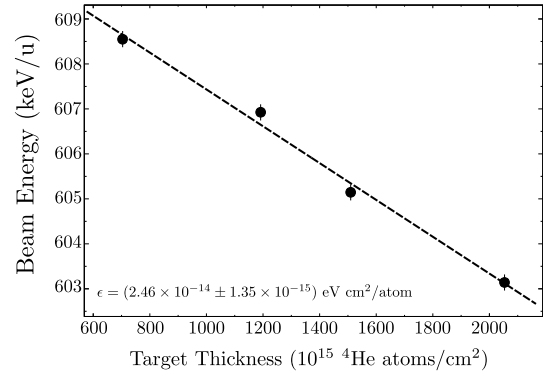


Figure 5: Gas target thickness versus beam energy for different values of the target pressure. The slope of the linear fit is the stopping power ϵ .

is excited upstream of the center of the gas target, indicating that the resonance energy is higher than 1458.5 keV. Therefore, we cannot use the standard method of DRAGON to determine the resonance energy from the distribution of the z position of the highest energy γ ray, since it assumes that the resonance is excited in the uniform density region surrounding the center of the gas target [18]. Instead, we performed a likelihood analysis similar to the ones in References [19, 20] to extract the resonance energy E_r , and its strength $\omega\gamma$.

To begin, we performed simulations for the z distribution of the highest energy γ rays using different resonance energies (13 values, spanning from $E_r = 1457.8$ to 1469.8 keV) and a fixed beam energy of 3.675 MeV and spread equal to the experimental one, with the standard DRAGON GEANT3 simulation package¹ [21]. The GEANT input file included nuclear level information, such as lifetimes and γ branching ratios, from Reference [22]. For the γ ray angular distribution, which as we discussed earlier affects the recoil transmission through the separator, we proceeded as follows: a spin 1 beam (^6Li) on a spin 0 target (^4He) can populate $M = 0, \pm 1$ magnetic substates of ^{10}B . Using Reference [23], we found the statistical tensor coefficients $\rho_2(2, 0) = \rho_2(2, 1) = -1.195$. Then we multiplied with the geometry factors $R_2(2 \rightarrow 3) = 0.1195$ and $R_2(2 \rightarrow 1) = 0.4183$, which results in the γ angular distribution for the two transitions: $W(\theta) = 0.86 + 0.21 \sin^2(\theta)$ to the $J = 3$ ground state and $W(\theta) = 0.5 + 0.75 \sin^2(\theta)$ to the $J = 1$ first excited state. Therefore the angular distribution of the dominant ground state transition is nearly

¹The GEANT3 simulation package of DRAGON can be found at https://github.com/DRAGON-Collaboration/G3_DRAGON

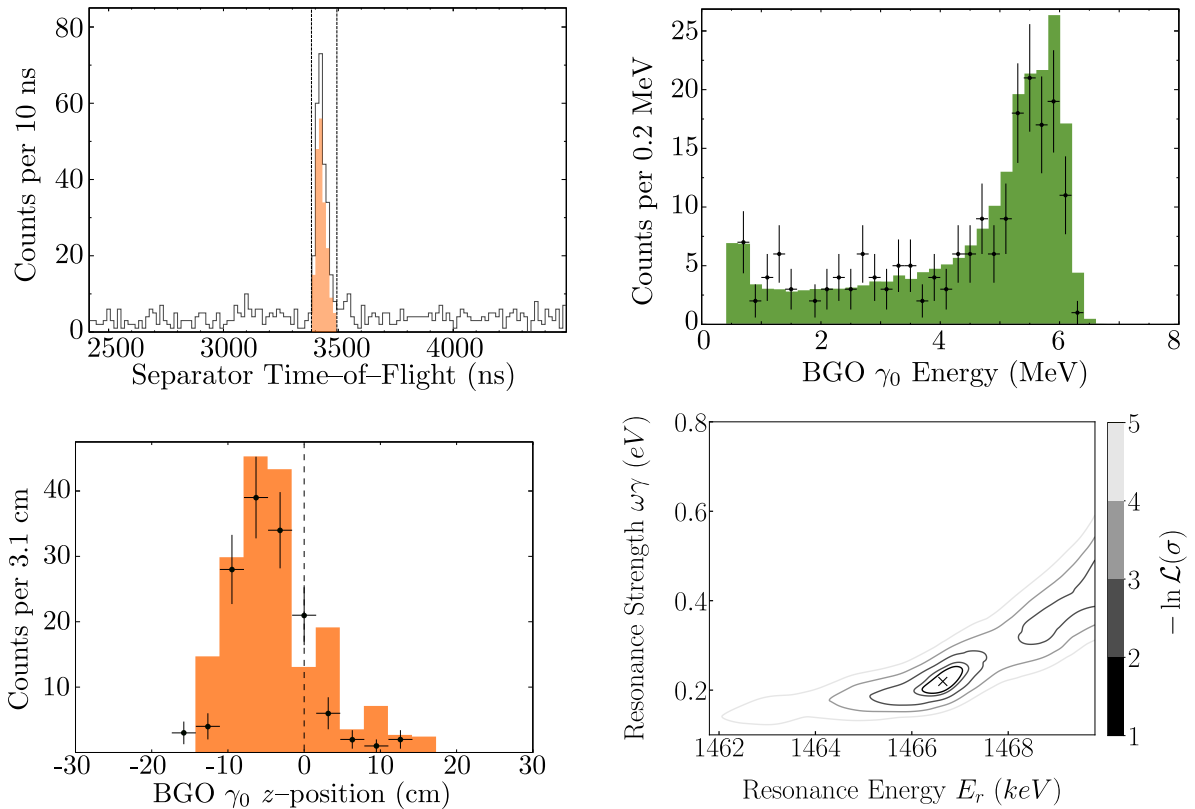


Figure 6: (Colour online) (Top Left) Separator time-of-flight spectrum for particle identification. The gate shown is for $\tau = 3.38 - 3.49 \mu\text{s}$. (Top Right) γ_0 energy plot comparison between experiment (black points) and GEANT simulation (green histogram). Both transitions of the $E_r = 1458.5$ keV resonance can be seen. (Bottom Left) The distribution of the z -position of the highest energy γ ray for a yield measurement at $P=5$ Torr. The centroid is at -3.85 cm from the center of the gas target. The orange histogram shows the global best fit by means of GEANT simulations (Bottom Right) Negative Log-likelihood contour plot for the $(E_r, \omega\gamma)$ space. The grey cross shows the minimum. See the text for a detailed discussion.

isotropic and that of the other is between isotropic and bipolar.

In addition, we took into account the transmission of the beam through the gas target. In particular, during the experiment we measured an $\sim 86\%$ transmission of the beam through the gas target by means of Faraday cup measurements. This implies that the beam was not centered as it was entering the gas target, given that its $2\times\text{rms}$ size, assuming a Gaussian profile, was measured by the ISAC operators to be 1.78 mm in both x and y . To include this piece of information in our GEANT simulations, we performed Monte-Carlo simulations sampling both x - and y -axis offsets for the measured beam size. Figure 7 shows the results of the simulated transmission. After that, we selected six point with 86% transmission to perform our simulations (black points in Figure 7).

We then scaled the generated BGO spectra according

to the expected reaction yield by a factor

$$\eta \frac{Y_{\omega\gamma_0} N_{beam}}{N_{sim}}, \quad (5)$$

where η is the recoil detection efficiency², $Y_{\omega\gamma_0}$ is the reaction yield from a single-level Breit-Wigner resonance ($\Gamma = 5.82$ keV [22]) of arbitrary strength $\omega\gamma$ (200 values spanning from $0.05 - 10$ eV), N_{beam} is the number of incident beam ions (See Section 5.2) and $N_{sim} = 5 \times 10^4$ is the number of simulated events. The BGO array γ ray detection efficiency η_{BGO} and the separator transmission $\eta_{separator}$ are built-in the GEANT simulation, and thus we do not include them in the η factor. The simulated γ spectra are convoluted with a Gaussian resolution function with $\sigma(E) = 0.1733 \sqrt{E}/(\ln 2 \sqrt{8})$, which is based on the experimentally measured resolution of the BGO array. The scaled BGO spectra are

²It includes the recoil charge state fraction, the heavy ion detector efficiency, and the data acquisition dead time.

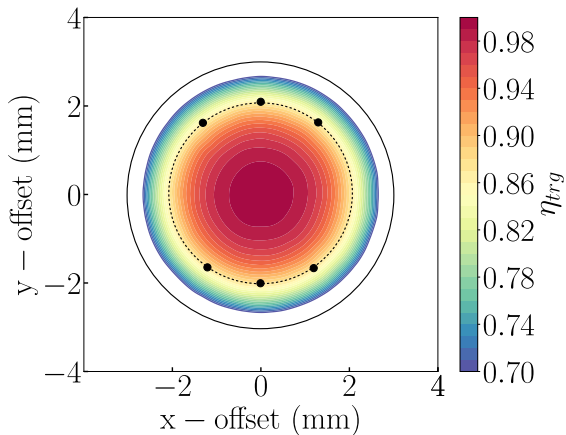


Figure 7: (Colour online) Beam transmission results for a beam with $2\times$ rms size of 1.78 mm in x- and y-axis. The black points show the locations selected for additional GEANT simulations. See the text for details.

then compared to the experimental data. From these simulations we created a $(E_r, \omega\gamma)$ space of 2,600 points (13×200) and for each point on this grid, we calculated the negative log-likelihood using:

$$-\ln\mathcal{L} = \sum_i [\ln(n_i!) - n_i \ln(f_i)] + S, \quad (6)$$

where i is the number of bins in the experimental BGO spectrum, n_i is the number of events in the i^{th} bin, f_i is the number of events in the scaled simulation i^{th} bin and S the total number of events in the scaled histogram.

Table 3: Settings of the GEANT3 simulation for the Log-Likelihood analysis. Nuclear properties were adopted from Reference [22]. See the text for details.

Quantity	Used Value
Excited state lifetime	1.13×10^{-19} s
Resonance energy	1457.8–1469.8 keV
Beam mass excess	14.087 MeV
Recoil mass excess	12.051 MeV
α partial width	5.82 keV
γ partial width	0.1114 eV
γ branching ratios	82% (to the ground state) 18% (to the first excited)
γ angular distributions	
$2 \rightarrow 3$ (ground state)	$W(\theta) = 0.86 + 0.21 \sin^2(\theta)$
$2 \rightarrow 1$ (first excited)	$W(\theta) = 0.50 + 0.75 \sin^2(\theta)$

Figure 6 shows the results of our simulations with a single minimum for the negative log-likelihood, with

energy that corresponds to a location inside the gas target. The global minimum has $-\ln\mathcal{L}_0 = 35.69$ and it is the only point where a 1σ contour can be deduced.

On top of the above analysis, we also performed tests on the GEANT simulation by changing the random seed of the Monte Carlo simulation, to ensure that the distribution of events is Poissonian, as in an experimental study. Due to the large number of simulation events ($N_{sim} = 5 \times 10^4$) the final result does not depend on the random seed.

The sources of systematic uncertainty in the final result for the resonance strength are presented in Table 4. The most important source of systematic uncertainty is the BGO efficiency which accounts for 11.4% and it was determined by varying the γ branching ratios of the resonance. The statistical uncertainty originates from the Log-Likelihood analysis and is defined by the bounds of the 1σ contour ($\delta\omega\gamma = {}^{+0.025}_{-0.035}$ eV) For the level excitation energy, E_x , we have similarly taken into account the statistical uncertainty from the Log-Likelihood analysis, ± 0.5 keV, and for the systematic uncertainty, we adopt the relative uncertainty of the beam energy $\delta E_{beam} = 0.16\%$, which yields $\delta E_x(\text{syst.}) = 2.4$ keV.

Table 4: Relative systematic uncertainties used to calculate the resonance strength of the $E_r = 1458.5$ keV resonance.

Quantity	Measured Value	Relative Uncertainty
η_{CSF}	0.523(8)	1.5%
N_{beam}	$3.252(53) \times 10^{14}$	1.64%
η_{BGO}	0.332(38)	11.4%
$\eta_{separator}$	0.122(5)	4.1%
ϵ (eV cm ²)	$24.63(136) \times 10^{15}$	5.5%
$\eta_{lifetime}$	0.91573(8)	0.009%
E_{beam} (A MeV)	0.612(1)	0.16%
Total systematic uncertainty		13.49%

The results for the resonance energy E_r , excitation energy E_x and strength $\omega\gamma$, for this minimum are the following:

$$E_r = 1466.6 \pm 0.5 (\text{stat.}) \pm 2.4 (\text{syst.}) \text{ keV}$$

$$E_x = 5927.8 \pm 0.5 (\text{stat.}) \pm 2.4 (\text{syst.}) \text{ keV}$$

$$\omega\gamma = 0.225 {}^{+0.025}_{-0.035} (\text{stat.}) \pm 0.030 (\text{syst.}) \text{ eV}$$

Our final resonance strength is in excellent agreement with the measurement of Forsyth *et al.* [9] as shown in

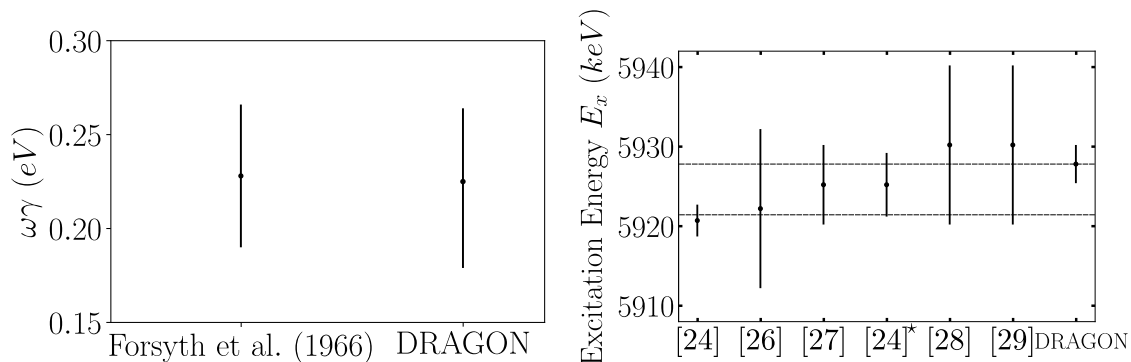


Figure 8: (Left) Comparison between the result of Forsyth *et al.* and the present work for the resonance strength of the $E_r = 1458.5$ keV resonance. (Right) Excitation energies for the $E_x = 5919.5$ keV state of ^{10}B from normalized literature values (Table 6) compared with the present work. The bands correspond to the EVM average uncertainty. See the text for a detailed discussion.

Figure 8. However, the resonance energy (excitation energy) we extracted with DRAGON is higher than the recommended value in nuclear databases [24]. A literature search (References [25, 26, 27, 28, 29, 29, 30]) shows that the excitation energy E_x , for the state of interest lies between 5920–5930 keV, which is consistent with our result (see Table 6 and Figure 8). To obtain an average literature–based excitation energy with a realistic uncertainty, we first excluded the measurement of Buccino & Smith [26] as an outlier ($E_x = 5900 \pm 80$ keV) applying Peirce’s criterion [31]. We then calculated the average using the Expected Value Method (EVM) [32] for all the remaining measurements with reported uncertainties to be $E_x = (5920.3 \pm 2.4)$ keV. It is worth mentioning that the adopted level energy of $E_x = (5919.5 \pm 0.6)$ keV [24] is mainly determined by the high–precision measurement reported in Reference [25]. However, this result was extracted using an Enge split–pole spectrograph which usually results in excitation energy uncertainties of approximately ± 5 keV [33]. For this reason, we also calculated the EVM average with a more realistic uncertainty for the study of Reference [25], based on their analysis $-\delta E_x = 2$ keV — to be $E_x = (5921.2 \pm 3.2)$ keV. Furthermore, we investigated how the reaction Q value changed between the literature measurements. We found a $\sim 1 - 2$ keV difference between the $A = 10$ evaluations and the AME2016 compilation, which we used for our calculations [12, 22, 34, 35, 36, 37, 38, 39] (see also Table 5). In particular, the Q value changes between the 1979 to 1984 and 1984 to 1988 evaluations are based on mass measurements reported in References [40] and [41], respectively. For this reason, we adjusted the literature values of the excitation energy to the current Q value, assuming that they were following the latest

$A = 10$ evaluation at the time of publication (see Table 6). The new result, $E_x = (5924.6 \pm 3.2)$ keV agrees within 1σ with the energy extracted using the Negative Log–Likelihood analysis $E_x = 5927.8 \pm 0.5$ (*stat.*) ± 2.4 (*syst.*) keV (see Figure 8).

Table 5: Evolution of the $^6\text{Li}(\alpha, \gamma)^{10}\text{B}$ reaction Q value through the years. See the text for details.

Year	Q value (keV)	ΔQ (keV)	Ref.
2017	4461.19	-	[12]
2004	4461.10	+0.09	[22]
1988	4459.60	+1.59	[39]
1984	4460.30	+0.89	[38]
1979	4460.50	+0.69	[37]
1974	4460.00	+1.19	[36]
1966	4461.00	+0.19	[35]
1959	4459.00	+2.19	[34]

6. Discussion & Conclusions

As this work demonstrates, such measurements can provide a test of the limits of the DRAGON angular acceptance, using a known resonance of the $^6\text{Li}(\alpha, \gamma)^{10}\text{B}$ reaction. It is worth noting that such measurements can provide reliable results only if they are coupled with detailed simulations of the separator, which provide the important information on the recoil transmission and the γ ray detection efficiency. The data analysis is also affected by our knowledge of the γ branching ratios and angular distributions $W(\theta)$, as discussed in Section 2. Accurate measurements of the γ branching ratios using high efficiency detectors are desirable, but even if they are unknown, the γ ray detection efficiency can still be

Table 6: Summary of reported energies for the $E_x = 5920$ keV state of ^{10}B from different measurements, normalized to the current $^6\text{Li}(\alpha, \gamma)^{10}\text{B}$ reaction Q value [12]. See the text for a detailed discussion.

Reaction	E_x (keV)	δE_x (keV)	Reference
$^9\text{Be}(d, n)^{10}\text{B}$	5902.2	80	Buccino & Smith [26]
$^{10}\text{B}(p, p')^{10}\text{B}$	5920.7	0.6	Kashy, Benenson & Nolen Jr. [25]
$^{10}\text{B}(d, d')^{10}\text{B}$	5922.2	10	Armitage & Meads [27]
$^{10}\text{B}(p, p')^{10}\text{B}$	5922.2	10	Armitage & Meads [27]
$^{11}\text{B}(^3\text{He}, \alpha)^{10}\text{B}$	5925.2	5	Gorodetzky <i>et al.</i> [28]
N/A	5925.2	4	Reported in Reference [25]
$^9\text{Be}(d, n)^{10}\text{B}$	5930.2	10	Yong Sook <i>et al.</i> [29]
$^9\text{Be}(d, n)^{10}\text{B}$	5930.2	10	Fife <i>et al.</i> [30]
Average	5921.3	3.2	Without normalized Q value
Average	5924.6	3.2	With normalized Q value
$^6\text{Li}(\alpha, \gamma)^{10}\text{B}$	5927.8	± 0.5 (stat.) ± 2.4 (syst.)	DRAGON

calculated using a combination of the experimental data and simulations [1]. The final result, however, might suffer from higher systematic uncertainty.

The results we obtained in this work are in excellent agreement with the only known measurement by Forsyth *et al.*, showing that DRAGON can measure resonance strengths of reactions with large recoil angular cones. We can now proceed with confidence to study a wide range of alpha-capture reactions (see Table 1), previously thought inaccessible with DRAGON due to recoil acceptance constraints. This includes a planned measurement of the $^7\text{Be}(\alpha, \gamma)^{11}\text{C}$ reaction at energies relevant to νp -process nucleosynthesis.

Acknowledgements

The authors gratefully acknowledge the beam delivery and ISAC operations groups at TRIUMF. The core operations of TRIUMF are supported via a contribution from the federal government through the National Research Council of Canada, and the Government of British Columbia provides building capital funds. DRAGON and authors from McMaster University are receive funds from the National Sciences and Engineering Research Council of Canada (NSERC). A.P. thanks Greg Christian (St. Mary’s University) for valuable discussions concerning the GEANT simulations, and the anonymous reviewers whose comments/suggestions helped improve and clarify this manuscript. Authors from the UK are supported by the Science and Technology Facilities Council. Authors from Colorado School of Mines acknowledge support from U.S. Department of Energy Office of Science DE-FG02-93ER40789 grant. This work benefited from discussions at the “Nuclear

Astrophysics at Rings and Recoil Separators” Workshop supported by the National Science Foundation under Grant No. PHY-1430152 (JINA Center for the Evolution of the Elements).

References

- [1] C. Ruiz, U. Greife, U. Hager, Recoil separators for radiative capture using radioactive ion beams, *The European Physical Journal A* 50 (2014) 99.
- [2] C. R. Brune, B. Davids, Radiative capture reactions in astrophysics, *Annual Review of Nuclear and Particle Science* 65 (2015) 87–112.
- [3] D. Hutcheon, S. Bishop, L. Buchmann, M. Chatterjee, A. Chen, J. D’Auria, S. Engel, D. Gigliotti, U. Greife, D. Hunter, et al., The DRAGON facility for nuclear astrophysics at TRIUMF-ISAC: design, construction and operation, *Nuclear Instruments and Methods in Physics Research Section A: Accelerators, Spectrometers, Detectors and Associated Equipment* 498 (2003) 190–210.
- [4] C. Vockenhuber, L. Buchmann, J. Caggiano, A. Chen, J. D’Auria, C. Davis, U. Greife, A. Hussein, D. Hutcheon, D. Ottewell, et al., Improvements of the dragon recoil separator at ISAC, *Nuclear Instruments and Methods in Physics Research Section B: Beam Interactions with Materials and Atoms* 266 (2008) 4167–4170.
- [5] S. Sjøe, B. N. Singh, P. Adsley, L. Buchmann, M. Carmona-Gallardo, B. Davids, J. Fallis, B. Fulton, N. Galinski, U. Hager, et al., Beam suppression of the dragon recoil separator for $^3\text{He}(\alpha, \gamma)^7\text{Be}$, *Nuclear Instruments and Methods in Physics Research Section A: Accelerators, Spectrometers, Detectors and Associated Equipment* 700 (2013) 179–181.
- [6] J. Fallis, C. Akers, A. Laird, A. Simon, A. Spyrou, G. Christian, D. Connolly, U. Hager, D. Hutcheon, A. Lennarz, et al., First measurement in the gamow window of a reaction for the γ -process in inverse kinematics: $^{76}\text{Se}(\alpha, \gamma)^{80}\text{Kr}$, *Physics Letters B* 807 (2020) 135575.
- [7] D. Lehbertz, S. Courtin, F. Haas, D. Jenkins, C. Simenel, M.-D. Salsac, D. Hutcheon, C. Beck, J. Cseh, J. Darai, et al., $^{12}\text{C}(^{16}\text{O}, \gamma)^{28}\text{Si}$ radiative capture: Structural and statistical aspects of the γ decay, *Physical Review C* 85 (2012) 034333.

- [8] C. Matei, L. Buchmann, W. Hannes, D. Hutcheon, C. Ruiz, C. Brune, J. Caggiano, A. Chen, J. D'Auria, A. Laird, et al., Measurement of the Cascade Transition via the First Excited State of ^{16}O in the $^{12}\text{C}(\alpha, \gamma)^{16}\text{O}$ Reaction, and Its S Factor in Stellar Helium Burning, *Physical review letters* 97 (2006) 242503.
- [9] P. Forsyth, H. Tu, W. Hornyak, The $^6\text{Li}(\alpha, \gamma)^{10}\text{B}$ reaction and the energy levels of ^{10}B , *Nuclear Physics* 82 (1966) 33–48.
- [10] K. Jayamanna, F. Ames, G. Cojocaru, R. Baartman, P. Bricault, R. Dube, R. Laxdal, M. Marchetto, M. MacDonald, P. Schmor, et al., Off-line ion source terminal for ISAC at TRIUMF, *Review of Scientific Instruments* 79 (2008) 02C711.
- [11] L. Meyer-Schützmeister, S. Hanna, Energy levels in ^{10}B in the reaction $^6\text{Li}(\alpha, \gamma)^{10}\text{B}$, *Physical Review* 108 (1957) 1506.
- [12] M. Wang, G. Audi, F. Kondev, W. Huang, S. Naimi, X. Xu, The AME2016 atomic mass evaluation (II). Tables, graphs and references, *Chinese Physics C* 41 (2017) 030003.
- [13] R. Laxdal, Acceleration of radioactive ions, *Nuclear Instruments and Methods in Physics Research Section B: Beam Interactions with Materials and Atoms* 204 (2003) 400–409.
- [14] G. Christian, C. Akers, D. Connolly, J. Fallis, D. Hutcheon, K. Olchanski, C. Ruiz, Design and commissioning of a timestamp-based data acquisition system for the DRAGON recoil mass separator, *The European Physical Journal A* 50 (2014) 75.
- [15] D. Hutcheon, L. Buchmann, A. Chen, J. D'Auria, C. Davis, U. Greife, A. Hussein, D. Ottewell, C. Ouellet, A. Parikh, et al., Background suppression by the DRAGON radiative capture facility at TRIUMF/ISAC, *Nuclear Instruments and Methods in Physics Research Section B: Beam Interactions with Materials and Atoms* 266 (2008) 4171–4175.
- [16] W. Liu, G. Imbriani, L. Buchmann, A. Chen, J. D'Auria, A. D'Onofrio, S. Engel, L. Gialanella, U. Greife, D. Hunter, et al., Charge state studies of low energy heavy ions passing through hydrogen and helium gas, *Nuclear Instruments and Methods in Physics Research Section A: Accelerators, Spectrometers, Detectors and Associated Equipment* 496 (2003) 198–214.
- [17] G. Schiwietz, P. Grande, Improved charge-state formulas, *Nuclear Instruments and Methods in Physics Research Section B: Beam Interactions with Materials and Atoms* 175 (2001) 125–131.
- [18] D. Hutcheon, C. Ruiz, J. Fallis, J. D'Auria, B. Davids, U. Hager, L. Martin, D. Ottewell, S. Reeve, A. Rojas, Measurement of radiative capture resonance energies with an extended gas target, *Nuclear Instruments and Methods in Physics Research Section A: Accelerators, Spectrometers, Detectors and Associated Equipment* 689 (2012) 70–74.
- [19] L. Erikson, C. Ruiz, F. Ames, P. Bricault, L. Buchmann, A. Chen, J. Chen, H. Dare, B. Davids, C. Davis, et al., First direct measurement of the $^{23}\text{Mg}(p, \gamma)^{24}\text{Al}$ reaction, *Physical Review C* 81 (2010) 045808.
- [20] G. Christian, G. Lotay, C. Ruiz, C. Akers, D. Burke, W. Catford, A. Chen, D. Connolly, B. Davids, J. Fallis, et al., Direct measurement of astrophysically important resonances in $^{38}\text{K}(p, \gamma)^{39}\text{Ca}$, *Physical Review C* 97 (2018) 025802.
- [21] D. G. Gigliotti, Efficiency calibration measurement and GEANT simulation of the DRAGON BGO gamma array at TRIUMF, Master's thesis, University of Northern British Columbia, Prince George, Canada, 2004.
- [22] D. Tilley, J. Kelley, J. Godwin, D. Millener, J. Purcell, C. Sheu, H. Weller, Energy levels of light nuclei $A = 8, 9, 10$, *Nuclear Physics A* 745 (2004) 155–362.
- [23] H. Rose, D. Brink, Angular distributions of gamma rays in terms of phase-defined reduced matrix elements, *Reviews of Modern Physics* 39 (1967) 306.
- [24] NuDat, 2.8 database <http://www.nndc.bnl.gov/nudat2/>, in: National Nuclear Data Center, Brookhaven National Laboratory (2020).
- [25] E. Kashy, W. Benenson, J. Nolen Jr, $A = 9$ isospin quartet, *Physical Review C* 9 (1974) 2102.
- [26] S. Buccino, A. Smith, Levels in ^{10}B excited by the $^9\text{Be}(d, n)$ reaction, *Physics Letters (Netherlands) Divided into Phys. Lett. A and Phys. Lett. B* 19 (1965).
- [27] B. Armitage, R. Meads, Levels in ^{10}B above 5.16 mev observed by proton and deuteron inelastic scattering, *Physics Letters* 8 (1964) 346–349.
- [28] S. Gorodetzky, A. Gallmann, R. Rebmeister, Study of the excited states of ^{10}B from 5 to 8 MeV by the $^{11}\text{B}(^3\text{He}, \alpha)^{10}\text{B}$ reaction and a note on the $^{11}\text{B}(^3\text{He}, t)^{11}\text{C}$ reaction, *Physical Review* 137 (1965) B1466.
- [29] Y. S. Park, A. Niiler, R. Lindgren, Spectroscopy of ^{10}B levels from the $^9\text{Be}(d, n)^{10}\text{B}$ reaction, *Physical Review C* 8 (1973) 1557.
- [30] A. Fife, G. Neilson, W. Dawson, The excited states of ^{10}B , *Nuclear Physics A* 91 (1967) 164–176.
- [31] B. Peirce, Criterion for the rejection of doubtful observations, *The Astronomical Journal* 2 (1852) 161–163.
- [32] M. Birch, B. Singh, Method of best representation for averages in data evaluation, *Nuclear Data Sheets* 120 (2014) 106–108.
- [33] C. Marshall, K. Setoodehnia, K. Kowal, F. Portillo, A. E. Champagne, S. Hale, A. Dummer, R. Longland, The focal-plane detector package on the tunl split-pole spectrograph, *IEEE Transactions on Instrumentation and Measurement* 68 (2018) 533–546.
- [34] F. Ajzenberg-Selove, T. Lauritsen, Energy levels of light nuclei. vi, *Nuclear Physics* 11 (1959) 1.
- [35] T. Lauritsen, F. Ajzenberg-Selove, Energy levels of light nuclei (vii). a= 5–10, *Nuclear Physics* 78 (1966) 1–176.
- [36] F. Ajzenberg-Selove, T. Lauritsen, Energy levels of light nuclei a= 5-10, *Nuclear Physics A* 227 (1974) 1–243.
- [37] F. Ajzenberg-Selove, Energy levels of light nuclei a= 5-10, *Nuclear Physics A* 320 (1979) 1–224.
- [38] F. Ajzenberg-Selove, Energy levels of light nuclei a= 5-10, *Nuclear Physics A* 413 (1984) 1–168.
- [39] F. Ajzenberg-Selove, Energy levels of light nuclei a = 5-10, *Nuclear Physics A* 490 (1988) 1–225.
- [40] A. Chalupka, H. Vonach, E. Huges, H. Scheerer, Precision measurement of the mass of ^{10}B , *Zeitschrift für Physik A Atoms and Nuclei* 310 (1983) 135–136.
- [41] R. Ellis, K. Sharma, R. Barber, S. Loewen, H. Duckworth, The precise atomic masses of ^{10}B and ^{11}B , *Physics Letters B* 141 (1984) 306–308.